J|A|C|S
ARTICLES
Published on Web 05/24/2006

Ligation-State Hydrogen Exchange: Coupled Binding and Folding Equilibria in Ribonuclease P Protein

Christopher H. Henkels† and Terrence G. Oas*

Contribution from the Department of Biochemistry, Box 3711, Duke University Medical Center, Durham, North Carolina 27710

Received November 5, 2005; E-mail: oas@biochem.duke.edu

Abstract: *Bacillus subtilis* ribonuclease P protein (P protein) is predominantly unfolded (D) at physiological pH and low ionic strength; however, small molecule anionic ligands (e.g., sulfate) directly bind to and stabilize the folded state (NL_2). Because the $D + 2L \leftrightarrow NL_2$ transition is experimentally two-state, high-energy states such as the singly bound, folded species (NL) and the unliganded folded species (N) are generally difficult to detect at equilibrium. To study the conformational properties of these ensembles, NMR-detected amide hydrogen exchange (HX) rates of P protein were measured at four sulfate (i.e., ligand) concentrations, a method we denote "ligation-state hydrogen exchange". The ligand concentration dependence of the HX rate of 47 residues was fit to a model with four possible HX pathways, corresponding to the local and/or global opening reactions from NL_2 and NL, the local opening of N, and the global opening of N to D. Data analysis permits the calculation of the residue-specific free energy of opening from each ensemble as well as the fractional amide HX flux through each pathway. Results indicate that the predominant route of HX is through the NL and N states, which represent only 0.45% and 0.0005% of the total protein population in 20 mM sodium sulfate, respectively. Despite the low population of N, a region of protected amides was identified. Therefore, exchange through unliganded forms must be accounted for prior to the interpretation of HX-based protein-interaction studies. We offer a simple test to determine if HX occurs through the liganded or unliganded form.

Introduction

At equilibrium, proteins are best characterized as structural ensembles composed of very large numbers of conformations.[1] Conformations that contain both small-scale deviations (e.g., bond vibrations) and large amplitude excursions (e.g., global unfolding transitions) from the average structure exist within the protein ensemble. Although not well represented within the native ensemble, high-energy conformations may play critical roles in protein function. One role for high-energy conformations is allosteric and/or ligand-based protein activation.[2−4] In such cases, the average unliganded protein conformation may not resemble the active or ligand-bound conformation. However, small populations of active conformations can often be sufficient to confer requisite ensemble-averaged activities. These high-energy states can be difficult to detect under equilibrium conditions by most methods. However, amide hydrogen exchange (HX) is a technique that can probe poorly populated states.[5−7] Indeed, the free energy of the conformational change leading to exchange (ΔG_{HX}) for some amides is equivalent to the global stability (ΔG_u) of the protein. Therefore, HX experiments can probe rare opening transitions such as global unfolding under native conditions.

This sensitivity of HX to poorly populated states represents a potential pitfall in the interpretation of HX-based protein binding studies. As pointed out recently for ribonuclease S and the c-Src SH3 domain,[8,9] many of the slowly exchanging amides observed in protein−ligand complexes do so through the dissociated form of the protein, not the complex. Thus, HX patterns can be very misleading predictors of the location of protein−ligand interfaces if such amides are included in the analysis. Fortunately, as described here, these amides can be distinguished from those that exchange through the liganded protein complex by their unique ligand concentration dependence.

Bacillus subtilis ribonuclease P protein (P protein) is the protein subunit of the ribozyme RNase P, an essential enzyme required for the processing of precursor t-RNA.[10−12] P protein is predominantly unfolded when purified to homogeneity at

† Present address: Department of Biochemistry and Molecular Genetics, Box 800733, University of Virginia Health Sciences Center, Charlottesville, VA 22908.

(1) Lindorff-Larsen, K.; Best, R. B.; Depristo, M. A.; Dobson, C. M.; Vendruscolo, M. *Nature* **2005**, *433* (7022), 128−32.
(2) Volkman, B. F.; Lipson, D.; Wemmer, D. E.; Kern, D. *Science* **2001**, *291* (5512), 2429−33.
(3) Koshland, D. E. *Proc. Natl. Acad. Sci. U.S.A.* **1958**, *44* (2), 98−104.
(4) Mulder, F. A.; Mittermaier, A.; Hon, B.; Dahlquist, F. W.; Kay, L. E. *Nat. Struct. Biol.* **2001**, *8* (11), 932−5.
(5) Clarke, J.; Itzhaki, L. S. *Curr. Opin. Struct. Biol.* **1998**, *8* (1), 112−8.
(6) Raschke, T. M.; Marqusee, S. *Curr. Opin. Biotechnol.* **1998**, *9* (1), 80−6.
(7) Englander, S. W. *Annu. Rev. Biophys. Biomol. Struct.* **2000**, *29*, 213−38.
(8) Chakshusmathi, G.; Ratnaparkhi, G. S.; Madhu, P. K.; Varadarajan, R. *Proc. Natl. Acad. Sci. U.S.A.* **1999**, *96* (14), 7899−904.
(9) Wildes, D.; Marqusee, S. *Protein Sci.* **2005**, *14* (1), 81−8.
(10) Hsieh, J.; Andrews, A. J.; Fierke, C. A. *Biopolymers* **2004**, *73* (1), 79−89.

10.1021/ja057279+ CCC: $33.50

physiological pH and low ionic strength.[13] Therefore, P protein is classified as an intrinsically unstructured protein.[14,15] However, high-resolution structures of bacterial P protein have been solved, and P protein has been shown to adopt a compact, nearly spherical mixed α/β conformation.[16−18] Therefore, the favored P protein conformational ensemble is solution dependent, and the unfolded state can be induced to fold into the mixed α/β structure upon the addition of small anionic ligands such as sulfate.[13] Moreover, ligand-induced P protein folding is an apparently two-state process indicating that other states along the coupled folding/binding pathway have higher energies than the two end states.[13] One such state is the unliganded, folded state of P protein. This high-energy ensemble is a poorly populated collection of conformations that lack favorable folding enthalpy to compensate for the large entropy loss that opposes protein folding.[19] As a potential precursor to the assembly of the ribonucleoprotein complex that constitutes RNase P holoenzyme, the conformational and energetic properties of this state are of intrinsic biological interest. In this study we carried out amide HX experiments at various sodium sulfate (i.e., ligand) concentrations, a method we propose to call ligation-state hydrogen exchange by analogy to the powerful native-state hydrogen exchange method.[20] We use ligation-state HX to study the intermediates in the P protein coupled folding and binding reaction. Furthermore, we analyze the ligand concentration dependence of the exchange rate to discern regions of protection within each intermediate.

Materials and Methods

Sample Preparation. Recombinant ^{15}N-labeled P protein (^{15}N−P protein) was overexpressed in *E. coli* (DE3) pLysS cells in M9 minimal media containing $^{15}NH_4Cl$ (1 g/L) as the sole nitrogen source. Protein purification was carried out as described previously.[13] The purity of ^{15}N P protein was validated by SDS-PAGE, analytical HPLC, and electrospray mass spectroscopic analyses. Sodium cacodylate (NaCac) and deuterium chloride (D, 99.5%, 37% w/w) were from Sigma Chemical (St. Louis, MO); sodium azide was from Fisher Scientific (Fair Lawn, NJ); sodium sulfate was from EM Science (Gibbstown, NJ). Deuterated chemicals D_2O (D, 99.9%), sodium deuterioxide (D, 99.5%, 30% w/w), and TMSP-d_4 were from Cambridge Isotope Laboratories (Andover, MA). Ultrapure urea was from Nacalai Tesque (Kyoto, Japan). Deuterated urea was prepared by repeated dissolving in D_2O followed by freeze-drying. All buffers contained 10 mM NaCac at either pH 6 for hydrated solutions or pH* 6 (uncorrected pH meter reading) for deuterated solutions. Furthermore, hydrated or deuterated acid and base were used accordingly to maintain the proper pH or pH*.

To prepare P protein stocks, the dry protein was dissolved in either a protiated buffer (for HX experiments followed by NMR) or deuterated buffer (for urea denaturation experiments followed by far-UV CD). The protein stocks were placed in a 37 °C water bath for 15 min to dissolve the protein, followed by centrifugation at 15 000 rpm for 5 min to pellet undissolved protein. The Edelhoch method[21,22] was used to quantify P protein concentration. All of the NMR samples initially contained 1−1.5 mM ^{15}N P protein, 10 NaCac (pH 6), 0.02% (w/v) sodium azide, 20 μg/mL TMSP, 90% H_2O/10% D_2O, and a specific sulfate concentration. All of the far-UV CD samples initially contained 5 μM (unlabeled) P protein, 10 mM sodium cacodylate (pH* 6), 0.02% (w/v) sodium azide in deuterated (≥99%) buffer, and a specific sulfate concentration. The four sulfate concentrations were 20 mM, 50 mM, 100 mM, and 200 mM.

Circular Dichroism (CD) Spectroscopy. Far-UV CD measurements were carried out on an Aviv model 202 CD spectrophotometer equipped with a stirred thermoelectric cell holder. Urea titrations of P protein were performed at 25 °C, and samples were allowed to equilibrate for 10−15 min prior to titration. The CD signal at 222 nm was monitored at increasing urea concentration using a mixing time of 1 min, a signal averaging time of 30 s, and a bandwidth set to 1 nm. The urea concentration was determined by refractive index,[23] and the raw CD signal was converted to mean residue ellipticity ($[\Theta]_{222}$). The resulting urea titration curves were fit to a two-state unfolding model assuming a linear free energy dependence on molar urea concentration.[23,24]

Hydrogen Exchange (HX) Experiments Followed by NMR Spectroscopy. The HX experiments were carried out at 25 °C on a Varian INOVA 600 MHz spectrometer using a triple resonance probe equipped with a z-field gradient coil. ^{15}N/^{1}H HSQC resonance assignments from P protein refolded in 20 mM Na_2SO_4 (Henkels, Chamberlin, Venters, and Oas, in preparation) were transferred to the spectra in these experiments. The ^{15}N and ^{1}H chemical shift assignments are given in Table S1 of the Supporting Information. (No significant changes were observed in the HSQC spectra at different sulfate concentrations or in deuterated solutions.) The spectral windows were set to 10 000 and 850 Hz for the ^{1}H-dimension and the ^{15}N-dimension, respectively. The smaller spectral window in the indirect dimension aliased 14 backbone amide cross-peaks as well as a number of unassigned side chain resonances. However, aliased spectra had no resonance overlap. HSQC spectra were recorded with 2048 × 74 complex points, and a 1.5 s recycle delay was used for each spectrum. Four HSQCs with differing signal-to-noise ratios were collected prior to each HX reaction; 2, 4, 8, or 16 transients were used per increment in the ^{15}N-dimension. The corresponding data collection times were ∼4.25 min, ∼8.5 min, ∼16.5 min, or ∼33 min per HSQC.

Prior to the HX reaction, Sephadex G-25 resin (Amersham Biosciences, Uppsala, Sweden) was poured into an unpacked PD-10 column (2 cm × 1.5 cm). The sizing column was equilibrated with deuterated buffer containing 10 mM NaCac (pH* 6), 0.02% sodium azide, and the specific Na_2SO_4 concentration. HX was initiated (time set to 0 min) when the pre-exchange NMR sample was loaded onto the column. A 750 μL aliquot of the hydrated sample was loaded onto the deuterated column, followed by an 800 μL column wash and a subsequent 900 μL elution with deuterated buffer. The exchanged sample was transferred back into an NMR tube and placed into the spectrometer, and the magnet was shimmed as quickly as possible prior to collecting the first HSQC spectrum. Approximately 6 min elapsed between the initiation of the HX reaction and the collection of the first spectrum. HSQC spectra were collected in succession over various time scales ranging from 12 h (20 mM Na_2SO_4) to 2 days (200 mM Na_2SO_4). The shortest HSQC sampling rate was used for the first 20 spectra in all four HX reactions. Subsequent collection times were varied based

(11) Altman, S.; Kirsebom, L. In *The RNA World*, 2nd ed.; Gesteland, R. F., Cech, T. R., Atkins, J. F., Eds.; CSH Press: Cold Spring Harbor, NY, 1999; pp 351−80.
(12) Frank, D. N.; Pace, N. R. *Annu. Rev. Biochem.* **1998**, *67*, 153−80.
(13) Henkels, C. H.; Kurz, J. C.; Fierke, C. A.; Oas, T. G. *Biochemistry* **2001**, *40* (9), 2777−89.
(14) Tompa, P. *TRENDS in Biochemical Sciences* **2002**, *27* (10), 527−533.
(15) Dunker, A. K.; et al. *J. Mol. Graphics Modell.* **2001**, *19* (1), 26−59.
(16) Stams, T.; Niranjanakumari, S.; Fierke, C. A.; Christianson, D. W. *Science* **1998**, *280* (5364), 752−5.
(17) Spitzfaden, C.; Nicholson, N.; Jones, J. J.; Guth, S.; Lehr, R.; Prescott, C. D.; Hegg, L. A.; Eggleston, D. S. *J. Mol. Biol.* **2000**, *295* (1), 105−15.
(18) Kazantsev, A. V.; Krivenko, A. A.; Harrington, D. J.; Carter, R. J.; Holbrook, S. R.; Adams, P. D.; Pace, N. R. *Proc. Natl. Acad. Sci. U.S.A.* **2003**, *100* (13), 7497−502.
(19) Henkels, C. H.; Oas, T. G. *Biochemistry* **2005**, *44* (39), 13014−26.
(20) Englander, S. W.; Mayne, L.; Bai, Y.; Sosnick, T. R. *Protein Sci.* **1997**, *6* (5), 1101−9.
(21) Schmid, F. X. In *Protein structure: a practical approach*, ed.; Creighton, T. E., Ed.; IRL Press: Oxford, 1989; pp 251−285.
(22) Edelhoch, H. *Biochemistry* **1967**, *6*, 1948−1954.
(23) Pace, C. N. *Methods Enzymol.* **1986**, *131*, 266−80.
(24) Santoro, M. M.; Bolen, D. W. *Biochemistry* **1988**, *27* (21), 8063−8.

on the apparent observed peak intensity decay. Overall, 38, 59, 119, and 121 HSQCs were collected for the HX reactions containing 20 mM, 50 mM, 100 mM, and 200 mM Na_2SO_4, respectively.

All spectra were processed using NMRPipe.[25] The ^{1}H-dimension was zero-filled to 4096 points, while the ^{15}N-dimension was zero-filled to 148 points. Both dimensions were apodized with shifted sine-bell functions and Fourier transformed, and the amide proton region was extracted for a final 2048 (^{1}H) × 148 (^{15}N) matrix. Proper resonance phases were validated by nmrDraw.[25] Cross-peak intensities were calculated and tabulated with nmrView.[26]

To determine the rate constant of the HX reaction, the peak intensity for each cross-peak was initially normalized by the intensity of the corresponding pre-exchange cross-peak. The decay rate of the normalized peak intensity ratio, $I(t)$, was fit to the following two-parameter single-exponential equation:

$$I(t) = I(0)(e^{-k_{obs}t} + C) \quad (1)$$

$I(0)$ is the peak intensity ratio at zero time, k_{obs} is the HX rate constant, and C is a fixed constant corresponding to the *relative* peak intensity ratio at infinite time. Typically $I(\infty)$, the peak intensity ratio at infinite time, is allowed to float and not constrained to $I(0)$. However, we chose to fix $I(\infty)$ relative to $I(0)$ to avoid negative $I(\infty)$ values, which could yield inaccurate k_{obs} values. However, we initially fit a small number of decay curves containing significant time-independent exchanged baselines to the standard three-parameter single-exponential equation to estimate $I(\infty)$. The average C value ($C = I(\infty)/I(0)$) was determined for each sulfate reaction and corresponds to the fractional ^{1}H content in the exchanged sample solution. The fixed C constants were 0.057, 0.0582, 0.0523, and 0.0556 for the exchange reactions containing 20 mM, 50 mM, 100 mM, and 200 mM Na_2SO_4, respectively.

Analysis of HX Data. HX is a chemical reaction that requires solvent acid (H_3O^+ ion) or base (OH^- ion) to be in direct H-bonding contact with an exchanging amide hydrogen. Therefore, information about the structure of the native state ensemble can be inferred from differences between k_{obs} and k_{int}, the predicted HX intrinsic rate constant for the random-coil conformation.[5,6,20] The k_{int} values for P protein were derived from the model peptide studies of Bai et al.[27] The k_{obs} values are slower than k_{int} by several orders of magnitude for a subset of amides in a folded protein. The diminution in the relative exchange rate is caused by the presence of protein structure, which protects amides from solvent. Protection from exchange has been attributed to hydrogen-bonding and/or burial in the protein core.[28,29] Thus, some sort of conformational change is needed to facilitate HX at these sites.[30,31] Accordingly, the amide HX reaction can be modeled by Scheme 1.[32]

Scheme 1. Two-Step Model for Amide Hydrogen−Deuterium Exchange Reaction

$$NH_{cl} \underset{k_{cl}}{\overset{k_{op}}{\rightleftharpoons}} NH_{op} \xrightarrow{k_{int}} ND_{op}$$

NH_{cl} and NH_{op} represent the exchange-incompetent and the exchange-competent states. ND_{op} is the exchanged amide; the second step is effectively irreversible as the reaction is essentially in pure D_2O. The constants k_{op} and k_{cl} are the first-order rate constants defining the opening reaction and the closing reaction, respectively, while k_{int} is the pseudo-first-order rate constant defining the exchange reaction from the open state. In the so-called EX2 limit,[32] the closing rate constant is much faster than the intrinsic exchange rate constant, i.e., $k_{cl} \gg k_{int}$. Under these conditions, the observed pseudo-first-order rate constant describing the exchange of a particular amide (k_{obs}) can be related to the equilibrium constant of the opening reaction and the intrinsic rate constant:

$$k_{obs} = \frac{k_{op}}{k_{cl} + k_{op}} k_{int} = \frac{K_{op}}{1 + K_{op}} k_{int} = \frac{k_{int}}{PF_i} \quad (2)$$

where K_{op} is the equilibrium constant for the opening reaction and PF_i is the corresponding protection factor for residue i, which is equal to k_{int}/k_{obs}. The free energy change for the opening reaction ΔG_{HX} is obtained from K_{op}:

$$\Delta G_{HX} = -RT \ln K_{op} = -RT \ln\left(\frac{1}{PF_i - 1}\right) = -RT \ln\left(\frac{1}{\frac{k_{int}}{k_{obs}} - 1}\right) \quad (3)$$

Under EX2 conditions, HX experiments provide thermodynamic information on the opening reactions that lead to exchange. If the opening/closing reactions are assumed to correspond to conformational equilibria, then HX experiments can render information about poorly populated conformations within the native state ensemble.[7,20,33,34]

Results

Ligation-State Hydrogen Exchange of P Protein. To initiate the HX reaction, H_2O-equilibrated P protein was rapidly applied to a sizing column equilibrated with identical buffers made with D_2O, and the sample was subjected to a series of 10 min HSQC NMR spectra. Approximately 55 backbone resonances of the possible 115 were observed in the first spectrum. However, reliable exchange data could be extracted for 47 of these slow-exchanging, nonoverlapping resonances. As an example, Figure 1 shows the effect of sulfate concentration on the HX kinetics of T35 (β-strand 2). The decay rates for the normalized peak intensity ratios are well described by eq 1. The slight deviation at long time may be due to limited aggregation at higher sulfate concentrations, perhaps due to salting-out effects.[35] For many residues, the observed exchange rate is strongly dependent on sulfate concentration. For instance, the k_{obs} for T35 decreases from 0.0393 min^{-1} to 0.00113 min^{-1} as sulfate increases from 20 mM Na_2SO_4 to 200 mM Na_2SO_4. This corresponds to a nonlinear 35-fold increase in the protection factor (Figure 1, inset). The HX rates for the 47 resonances at all four ligand concentrations are listed in Table S2 (Supporting Information).

The assumption that HX occurs under at least partially EX2 conditions is supported by the observation that every resonance has an accelerated exchange rate in a control HX reaction at an elevated pH* of 6.7 (data not shown). Additionally, stopped-flow kinetics studies of a fluorescently labeled variant of P protein reveal an apparent rate constant ($k_{app} = k_u + k_f$) of ~10 s^{-1} at 20 mM sulfate and faster at higher sulfate concentrations (Y. Chang and T. G. Oas, in preparation). This rate constant is an order of magnitude faster than the fastest k_{int} for P protein. Thus, we assert that the EX2 limit applies to all of the collected data.

(25) Delaglio, F.; Grzesiek, S.; Vuister, G. W.; Zhu, G.; Pfeifer, J.; Bax, A. *J. Biomol. NMR* **1995**, *6* (3), 277−93.
(26) Johnson, B. A. *Methods Mol. Biol.* **2004**, *278*, 313−52.
(27) Bai, Y.; Milne, J. S.; Mayne, L.; Englander, S. W. *Proteins* **1993**, *17* (1), 75−86.
(28) Milne, J. S.; Mayne, L.; Roder, H.; Wand, A. J.; Englander, S. W. *Protein Sci.* **1998**, *7* (3), 739−45.
(29) Tuchsen, E.; Woodward, C. *J. Mol. Biol.* **1985**, *185* (2), 405−19.
(30) Englander, S. W.; Kallenbach, N. R. *Q. Rev. Biophys.* **1983**, *16* (4), 521−655.
(31) Woodward, C.; Simon, I.; Tuchsen, E. *Mol. Cell Biochem.* **1982**, *48* (3), 135−60.
(32) Hvidt, A.; Nielsen, S. O. *Adv. Protein Chem.* **1966**, *21*, 287−386.
(33) Li, R.; Woodward, C. *Protein Sci.* **1999**, *8* (8), 1571−90.
(34) Bai, Y.; Sosnick, T. R.; Mayne, L.; Englander, S. W. *Science* **1995**, *269* (5221), 192−7.
(35) Baldwin, R. L. *Biophys. J.* **1996**, *71* (4), 2056−63.

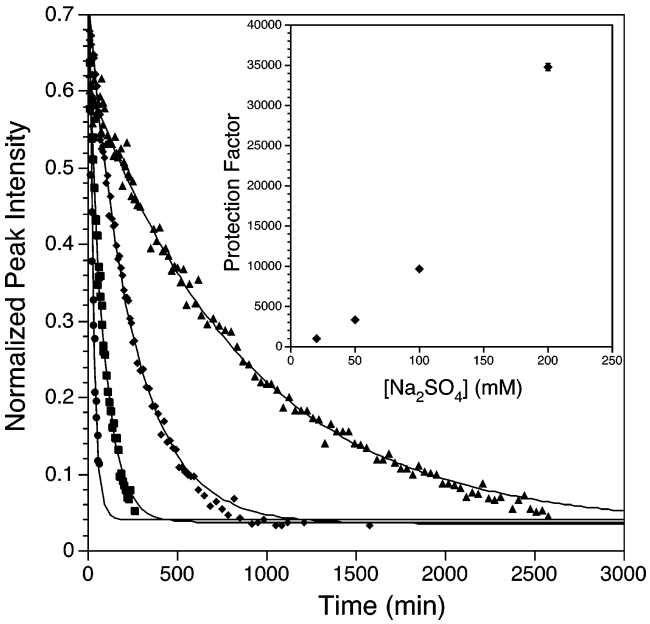

Figure 1. Effect of excess ligand on the observed HX rate, k_{obs}, of T35. The HX kinetics of T35 (β-strand 2) for P protein refolded in 20 mM (●), 50 mM (■), 100 mM (◆), and 200 mM (▲) Na_2SO_4 are shown. The lines through the exchange data represent the fits of the HX curves to a single-exponential equation (eq 1). The resulting sulfate dependence of the protection factor, $PF_{35} = k_{int}/k_{obs}$, for T35 is in the inset.

Figure 2 shows the apparent free energy change for the opening reaction of each the 47 observed residues, ΔG_{HX} calculated using eq 3. Several interesting qualitative observations are apparent in Figure 2. (1) Most of the protected amides reside in the secondary structure of P protein, with the distinct exception of α-helix 1. In fact, V26 (β-strand 1) is the first residue for which data are available. This is surprising because in the X-ray crystal structure most of the backbone amides in α-helix 1 have intramolecular H-bonds and are buried from solvent. However, the lack of protection suggests that α-helix 1, along with many of the loops, have exchange-competent conformations under native conditions.[36] (2) The protected residues do not correspond to the putative sulfate binding sites. The crystal structure of *B. subtilis* P protein revealed a sulfate coordinated by residues in the N-terminal region (H3 and R9) and α-helix 2 (R68).[16] Chemical-shift mapping of P protein in the presence of various small molecule ligands also implicates this region as an anion-binding site (Henkels, Chamberlin, Venters and Oas, in preparation). However, the N-terminal region readily exchanges with solvent (<6 min). Thus, the presence of sulfate does not appear to protect the backbone amides around its binding site. (3) The apparent global stability of P protein is ligand dependent. The overall protein stability, ΔG_u, increases from 4.7 ± 0.1 kcal/mol to 6.3 ± 0.2 kcal/mol over the observed sulfate range. Moreover, the global stabilities predicted from the thermodynamic parameters derived from CD thermal denaturation surface analysis[19] agree within error with the ΔG_u measured in this study by CD-detected urea denaturation. (4) The observed exchange rate constants decrease with increasing sulfate for every site that displays protection, reflected as an increase in ΔG_{HX} at higher sulfate. However, the *ligand dependence* of ΔG_{HX} is not uniform over the protein sequence (e.g., compare R29 and Y113). The lack of a uniform ligand dependence on k_{obs} suggests a plurality of opening pathways in the HX reaction (see below). Furthermore, there are a number of amides that appear to exchange "globally" based on the similarity of ΔG_{HX} and ΔG_u. However, as demonstrated below, we find that most of the HX occurs through opening reactions from the poorly populated singly liganded state (NL) or the free, folded state (N) and *not* from a global unfolding mechanism (D).

Fitting the Ligand Dependence of HX Rates to a Model with Four Exchange Pathways. The addition of sulfate greatly increases the protection of amides in P protein. This is not due to a significant increase in ligand binding to P protein (i.e., NL_2). The overall population of NL_2 rises from 99.96% to 99.998% over the sulfate concentration range used in this study. Note that these estimates were calculated assuming a two-state model for urea denaturation; specifically, that NL_2 and D are the *only* observable populations in the transition. However, the ligand concentration may affect the small population of the species that represents the primary route of HX. Since HX experiments are sensitive to these small populations, increased protection reflects the changes in these minute equilibrium populations. For example, there is a 7-fold reduction in the D population (0.04% to 0.006%) as the ligand concentration increases from 20 mM to 200 mM sulfate. This change would cause a significant reduction in the HX rate *if* exchange occurred primarily through D, because there would be less of this particular exchange-competent species at higher ligand concentration.[8,9,37,38] Thus, k_{obs} decreases as the population of the primary exchanging species is reduced; in other words, the ligand must dissociate in order for the dominant HX mechanism to occur.

The lack of a uniform ligand dependence of k_{obs} from residue to residue (Figure 2) indicates that more than one HX route exists for P protein in the presence of ligand. To properly account for the exchange through all of the possible routes, we have analyzed our results following the approach of Chakshusmathi et al.[8] and Wildes and Marqusee.[9] In both of these studies, the analysis assumed two possible pathways for HX, one route from the bound state (NL) and one route from the free state (N). By analogy, we have developed an HX reaction scheme (Scheme 2) that includes pathways through the doubly liganded, singly liganded, and unliganded forms of P protein.

As depicted in Scheme 2, HX of P protein in the presence of a ligand can occur through any one of six pathways involving the various liganded states of folded (N) and unfolded P protein (D). This scheme depicts global unfolding equilibria (to the left) to yield the open states D, DL, and DL_2 and the corresponding equilibrium constants: K_{glb}, K^{L}_{glb}, and K^{2L}_{glb}. Scheme 2 also depicts the interconversion of open and closed forms of N, NL, and NL_2 via local opening reactions (to the right), as described by residue-specific opening equilibrium constants: $K^{N}_{lcl,i}$, $K^{NL}_{lcl,i}$, and $K^{NL_2}_{lcl,i}$. It is important to recognize that these three equilibrium constants differ for each residue because a locally open

(36) Ferreon, J. C.; Volk, D. E.; Luxon, B. A.; Gorenstein, D. G.; Hilser, V. J. *Biochemistry* **2003**, *42* (19), 5582−91.
(37) Paterson, Y.; Englander, S. W.; Roder, H. *Science* **1990**, *249* (4970), 755−9.
(38) Mayne, L.; Paterson, Y.; Cerasoli, D.; Englander, S. W. *Biochemistry* **1992**, *31* (44), 10678−85.

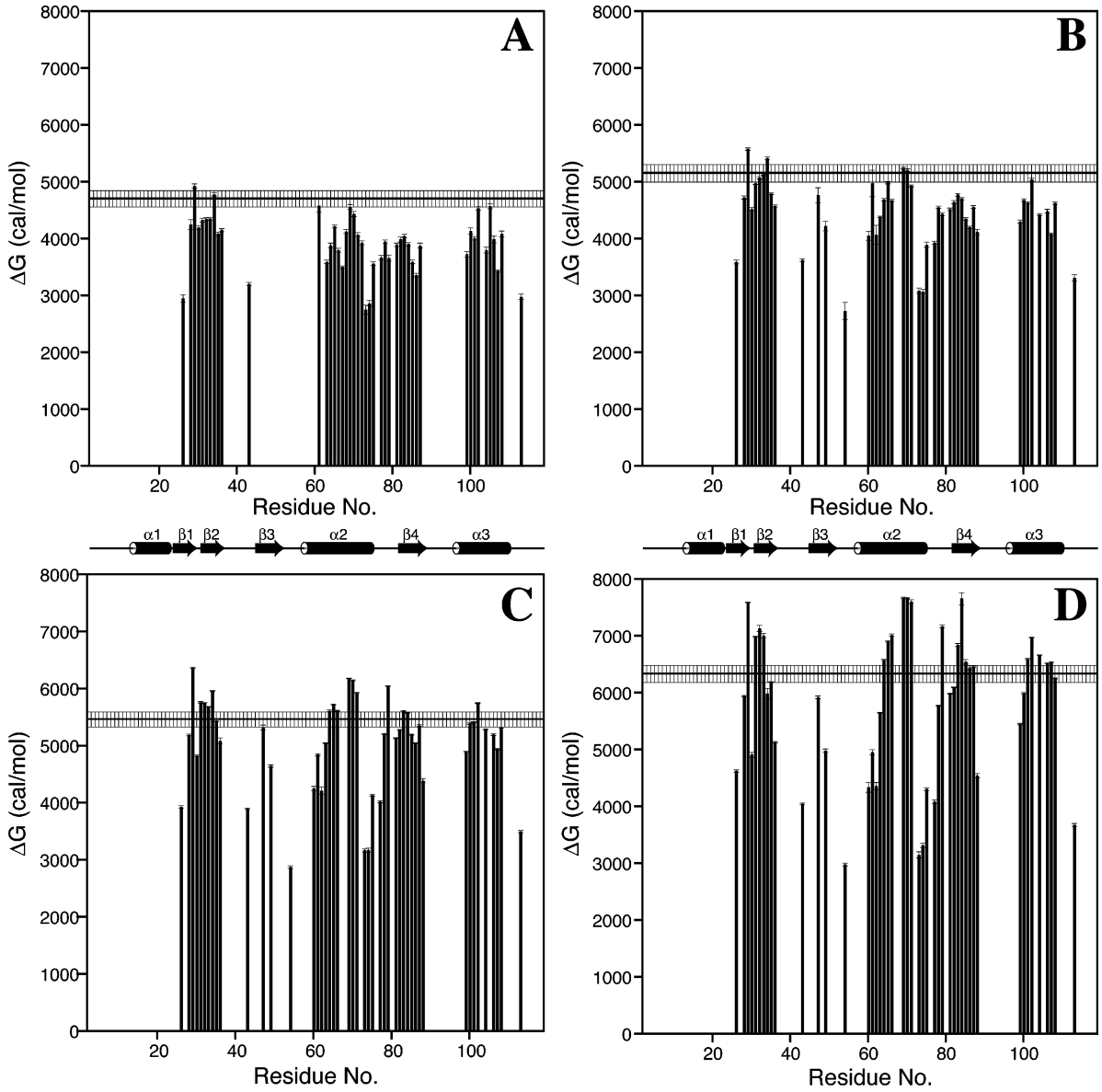

Figure 2. Effect of excess sulfate on HX rate for P protein. The k_{obs} for the 47 protected backbone amides were determined at four sulfate concentrations (Table S2). The ligand concentrations are (A) 20 mM, (B) 50 mM, (C) 100 mM, and (D) 200 mM Na_2SO_4. The resulting HX data were converted to the apparent free energy of opening, ΔG_{HX}, using eq 3; ΔG_{HX} values are shown as black bars. The black horizontal line is the global protein stability, ΔG_u, of P protein determined by urea titration followed by far-UV CD. The secondary structure derived from the *B. subtilis* crystal structure[16] is shown schematically above plots C and D.

Scheme 2. Model for P Protein HX Coupled to Folding and Binding

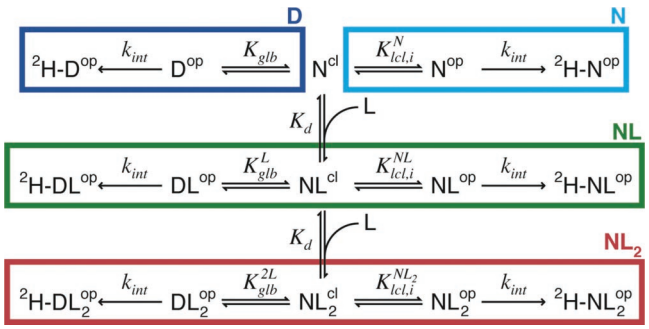

state (N^{op}, NL^{op}, or NL_2^{op}) is a different ensemble of conformations for each residue. Note that the two sulfate binding sites are assumed to be equivalent and independent. This simplifying assumption is supported by our previous studies of sulfate-induced folding of P protein.[13,19] The protection factor for the backbone amide hydrogen of residue *i*, PF_i, is the inverse of the fraction of conformations in which that amide is open or competent for exchange. Equation 4 gives PF_i in terms of the concentrations of the open and closed forms of the nine states shown in Scheme 2.

$$PF_i = \frac{[NL_2^{op}] + [NL^{op}] + [N^{op}] + [DL_2^{op}] + [DL^{op}] + [D^{op}] + [NL_2^{cl}] + [NL^{cl}] + [N^{cl}]}{[NL_2^{op}] + [NL^{op}] + [N^{op}] + [DL_2^{op}] + [DL^{op}] + [D^{op}]} \quad (4)$$

Under the assumption that the kinetics describing the opening and binding reactions are fast relative to k_{int}, the concentrations

in eq 4 can be expressed in terms of the equilibrium constants in Scheme 2. Expressing each concentration in terms of $[NL_2^{cl}]$ and then eliminating $[NL_2^{cl}]$ gives eq 5.

$$PF_i = \frac{K_{glb}^{2L} + K_{lcl,i}^{NL_2} + 2(K_{glb}^{L} + K_{lcl,i}^{NL})\frac{K_d}{[L]} + (K_{glb} + K_{lcl,i}^{N})\frac{K_d^{\,2}}{[L]^2} + 1 + \frac{2K_d}{[L]} + \frac{K_d^{\,2}}{[L]^2}}{K_{glb}^{2L} + K_{lcl,i}^{NL_2} + 2(K_{glb}^{L} + K_{lcl,i}^{NL})\frac{K_d}{[L]} + (K_{glb} + K_{lcl,i}^{N})\frac{K_d^{\,2}}{[L]^2}}$$

$$= 1 + \frac{\left(1 + \frac{K_d}{[L]}\right)^2}{K_{glb}^{2L} + K_{lcl,i}^{NL_2} + 2(K_{glb}^{L} + K_{lcl,i}^{NL})\frac{K_d}{[L]} + (K_{glb} + K_{lcl,i}^{N})\frac{K_d^{\,2}}{[L]^2}} \quad (5)$$

The factor of 2 in front of K_d/[L] terms accounts for the use of the microscopic binding constant, which assumes $K_d = K_d^{\alpha} = K_d^{\beta}$ for the α and β binding sites. Equation 5 can be simplified by eliminating the first term because experimentally measurable protection factors are much greater than one. Moreover, in the present experiments the ligand concentration is several orders of magnitude larger than the intrinsic K_d for sulfate, which makes the numerator of the second term ≈1. These simplifying approximations are equivalent to assuming that the ratio of closed to open states (PF_i) is the inverse of the sum of the open state populations. Making these simplifications in eq 5, and expressing it as the reciprocal, $1/PF_i$, gives a simple second-order polynomial in 1/[L]:

$$\frac{1}{PF_i} = (K_{glb}^{2L} + K_{lcl,i}^{NL_2}) + 2(K_{glb}^{L} + K_{lcl,i}^{NL})\frac{K_d}{[L]} + (K_{glb} + K_{lcl,i}^{N})\frac{K_d^{\,2}}{[L]^2} \quad (6)$$

Thus, a double reciprocal plot of $1/PF_i$ vs K_d/[L] displays ligation-state HX as a parabola whose shape can be fit to obtain the coefficients of each term in eq 6. Note that this analysis can yield only the aggregate opening equilibrium constants representing both local and global opening reactions:

$$\begin{aligned} K_{op}^{2L} &= K_{glb}^{2L} + K_{lcl,i}^{NL_2} \\ K_{op}^{L} &= K_{glb}^{L} + K_{lcl,i}^{NL} \\ K_{op} &= K_{glb} + K_{lcl,i}^{N} \end{aligned} \quad (7)$$

It is not possible to separate the local and global unfolding equilibrium constants for a given bound species from ligand concentration dependence alone, although studies that also included denaturant or osmolyte dependence would in principle allow the local and global contributions to be separated. For example, the unfolding equilibrium constant of the unliganded form of N (K_{glb}) has been previously estimated to be 35.5 at 25 °C,[19] which allows the value of $K_{lcl,i}^{N}$ to be estimated. After substitution of this value for K_{glb} and eq 7 into eq 6, the equation used for nonlinear least-squares fitting of the $1/PF_i$ vs K_d/[L] transformation of the data is

$$\frac{1}{PF_i} = K_{op,i}^{2L} + 2K_{op,i}^{L}\frac{K_d}{[L]} + (K_{lcl,i} + 35.5)\frac{K_d^2}{[L]^2} \quad (8)$$

The intrinsic microscopic dissociation constant for sulfate, K_d, has been previously determined to be 45 ± 2 μM at 25 °C from CD thermal denaturation surface analysis.[19] The resulting best-fit values for $K_{op,i}^{2L}$, $K_{op,i}^{L}$, and $K_{op,i}$, converted into free energy, are listed in Table 1, and typical fits are shown in Figure 3.

Table 1. ΔG_{op} from the NL_2, NL, and N States of P Protein

amino acid	ΔG_{op}^{2L} (kcal/mol)	ΔG_{op}^{L} (kcal/mol)	ΔG_{op} (kcal/mol)
V26		−0.1 ± 0.2	−3.4 ± 0.7
N28	6.2 ± 2.4	1.2 ± 0.6	−2.1 ± 1.6
R29	7.2 ± 4.2	2.5 ± 1.9	−2.1 ± 0.6
Q30	5.0 ± 0.3	1.4 ± 0.7	−2.1 ± 1.5
F31		1.5 ± 0.7	−2.4 ± 0.7
V32		1.6 ± 0.6	−2.5 ± 0.4
L33		1.7 ± 0.4	−2.6 ± 0.2
Y34	6.3 ± 0.6	2.2 ± 0.7	−2.1 ± 0.3
T35		1.3 ± 0.4	−2.7 ± 0.3
L36	5.5 ± 0.7	1.2 ± 0.6	−2.1 ± 1.8
E43	4.3 ± 0.1	0.1 ± 0.1	−2.1 ± 1.2
G47		1.4 ± 0.3	−3.1 ± 0.3
S49	5.7 ± 0.6	0.7 ± 0.1	−3.2 ± 0.3
I54	3.1 ± 0.1	−0.5 ± 0.2	−2.1 ± 2.0
R60	4.4 ± 0.4	1.2 ± 0.1	−3.4 ± 0.3
N61	5.0 ± 0.2		−2.2 ± 1.2
R62	4.5 ± 0.1	0.8 ± 0.5	−2.1 ± 6.9
I63		1.0 ± 0.3	−3.4 ± 0.1
K64		1.4 ± 0.8	−3.1 ± 0.3
R65		1.6 ± 0.6	−2.7 ± 0.3
L66		1.6 ± 1.0	−3.3 ± 0.2
Q69		1.9 ± 0.9	−2.3 ± 0.6
A70		1.9 ± 0.9	−2.6 ± 0.4
F71		1.9 ± 1.1	−3.0 ± 0.2
E73	3.2 ± 0.1		−4.1 ± 0.2
E74	3.3 ± 0.1	0.1 ± 0.1	−2.1 ± 1.2
K75	4.4 ± 0.2	0.6 ± 0.3	−2.1 ± 2.7
R77	4.1 ± 0.1	1.0 ± 0.1	−2.3 ± 0.3
L78		1.0 ± 0.4	−2.6 ± 0.7
K79		1.3 ± 1.7	−3.4 ± 0.5
K81		0.9 ± 0.4	−2.7 ± 0.7
D82		1.1 ± 0.4	−2.7 ± 0.5
Y83		1.4 ± 0.7	−2.9 ± 0.4
I84		1.4 ± 0.9	−3.1 ± 0.3
I85		1.0 ± 0.8	−3.4 ± 0.4
I86		1.0 ± 0.8	−3.7 ± 0.2
A87		1.1 ± 0.7	−2.9 ± 0.5
R88	4.7 ± 0.5	0.9 ± 0.1	−3.2 ± 0.3
T99		0.7 ± 0.3	−2.6 ± 0.9
K100		1.1 ± 0.5	−2.1 ± 1.6
K101		1.1 ± 0.6	−2.7 ± 0.8
S102		1.6 ± 0.9	−2.1 ± 1.3
Q104		0.9 ± 0.8	−2.9 ± 0.8
L106		0.9 ± 0.6	−2.1 ± 3.0
F107		0.7 ± 0.8	−3.4 ± 0.7
R108		1.0 ± 0.5	−2.2 ± 1.6
Y113	3.8 ± 0.1	−0.1 ± 0.2	−2.1 ± 5.0

Figure 3 depicts three classes of amides based on the K_d/[L] dependence of $1/PF_i$. Characteristic of the first class, Y113 and E43 have a statistically significant *y*-intercept, which represents the infinite ligand concentration limit. A nonzero *y*-intercept indicates the presence of HX through the fully liganded state, NL_2. Of the 47 residues, 17 have some portion of their HX through NL_2. The lack of curvature in the Y113 and E43 curves indicates that the remainder of the HX is through NL. I63 and I84 are representative amides for the second class of HX

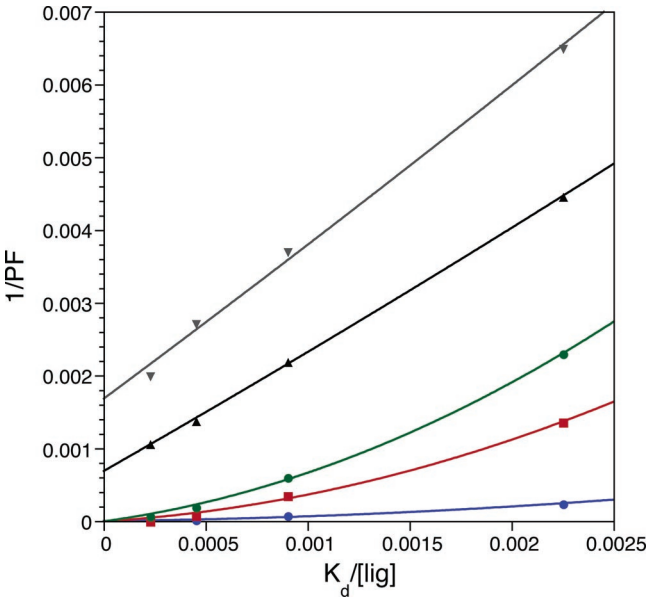

Figure 3. Representative double reciprocal plots of the ligand dependence of HX. The best-fit k_{obs} values are converted to PF^{-1} and plotted against K_d/[lig]. Data for Y113 (gray ▼), E43 (black ▲), I63 (green ●), I84 (red ■), and R29 (blue ●) are shown with the corresponding best-fit lines to eq 8 with the constraint $K^{2L}_{op,i}$, $K^{L}_{op,i}$, $K_{lcl,i} > 0$. The intrinsic dissociation constant for sulfate, K_d, was fixed to 45 μM.[19]

behavior. The lack of a significant *y*-intercept in Figure 3 suggests that these residues do not exchange from NL_2. Therefore, the principal routes of HX for these residues are through NL and N. The populations of these states are small at the saturating ligand concentrations studied here. As a result, the observed protection factors for these residues are high. Another distinguishing characteristic of this class is the apparent curvature shown in Figure 3. This curvature is due to a $1/[L]^2$ dependence caused by significant HX through the unliganded N state, which suggests that local fluctuations in this high energy intermediate state of P protein provide the preferable exchange route in the free state. R29 is an example of the last class of amides. Like I63 and I84, R29 is highly protected from exchange in the NL_2 state, but it also is protected in the NL state. Unlike I63 and I84, R29 shows low curvature in the double reciprocal plot in Figure 3. In fact, the best-fit value for ($K_{lcl,i}$ + 35.5) is approximately 35.5, indicating that there is little or no exchange at this residue through local opening of unliganded N. In other words, R29 is well protected in the high energy unliganded N state, and HX occurs only via global unfolding to the D state.

To determine the route by which a given amide exchanges, it is only necessary to compute its flux through the available opening pathways. The flux of reaction is calculated by multiplying the population of the reactant times the forward rate constant. Because k_{int} is assumed to be the same for all open states and independent of ligand concentration, the fractional flux of HX through a given pathway is equivalent to the fractional population of the corresponding open state, relative to all open states. The right side of eq 8 gives the sum of all open state populations. Thus, the fractional population of a particular open state is the population of that state divided by $1/PF_i$. Equations 9−12 describe the ligand concentration dependent fractional flux through the four HX pathways labeled NL_2, NL, N, and D in Scheme 2.

$$F_{NL_2}([L]) = K^{2L}_{op,i} PF_i([L]) \quad (9)$$

$$F_{NL}([L]) = 2K^{L}_{op,i} \frac{K_d}{[L]} PF_i([L]) \quad (10)$$

$$F_{N}([L]) = K_{lcl,i} \frac{K_d^2}{[L]^2} PF_i([L]) \quad (11)$$

$$F_{D}([L]) = 35.5 \frac{K_d^2}{[L]^2} PF_i([L]) \quad (12)$$

Figure 4 displays the fractional flux through each of the HX pathways in Scheme 2 at 20 mM and 200 mM Na_2SO_4. The fractional amide HX flux plots for P protein at all four ligand concentrations are shown in Figure S1 (Supporting Information). In the presence of 20 mM Na_2SO_4, the primary routes of HX are principally through two very poorly populated species, N (light blue bars) and NL (green bars). Based on the previously determined thermodynamic parameters,[19] the population of N is 5.0×10^{-6}, while the population of the NL is 0.0045 at this sulfate concentration. Additionally, several residues have a substantial portion (i.e., ≥20%) of their HX through the globally unfolded D state, which has a population of 1.8×10^{-4}.

It should be noted that for residues such as R29, which exchange primarily through N in 20 mM Na_2SO_4, the possibility that the exchange mechanism has some EX1 character is high. Kinetic studies indicate that the folding rate (k_{cl}) for the unliganded protein is ~1 s^{-1} (Chang and Oas, in preparation), which is comparable to typical k_{int} values. Under these conditions, the observed rate constant for NHex is likely to be lower than that under pure EX2 conditions, which would overestimate ΔG_{op} and thereby the flux through D instead of local opening from N. However, the total flux through the unliganded forms of the protein (sum of the blue bars in Figure 4) would be the same.

The fractional flux through the four pathways changes dramatically with increasing ligand concentration. In 200 mM Na_2SO_4, the primary routes of HX are through the bound states, NL and NL_2 (green and red bars, respectively). In this case, ligand has depopulated N and D to such an extent (5.0×10^{-8} and 1.8×10^{-6}, respectively) that exchange from the two bound states becomes predominant. Ligand can clearly modulate HX pathways even when the ligand concentration is significantly higher than the intrinsic dissociation constant. In the present case, the ligand concentration is 3−4 orders of magnitude higher than the 45 μM K_d for sulfate at 25 °C. Therefore, k_{obs} is extremely sensitive to ligand concentration even when the binding sites are saturated and the population of the bound state vastly exceeds that of any other component of the sample.

Discussion

Caution Is Required When Interpreting Alterations in HX Rate in the Presence and Absence of Ligand. HX detected by NMR spectroscopy is a commonly employed technique to map protein interaction sites.[37−47] In this technique, k_{obs} is

(39) Werner, M. H.; Wemmer, D. E. *J. Mol. Biol.* **1992**, *225* (3), 873−89.
(40) Benjamin, D. C.; Williams, D. C., Jr.; Smith-Gill, S. J.; Rule, G. S. *Biochemistry* **1992**, *31* (40), 9539−45.
(41) Orban, J.; Alexander, P.; Bryan, P. *Biochemistry* **1994**, *33* (19), 5702−10.
(42) Yi, Q.; Erman, J. E.; Satterlee, J. D. *Biochemistry* **1994**, *33* (40), 12032−41.

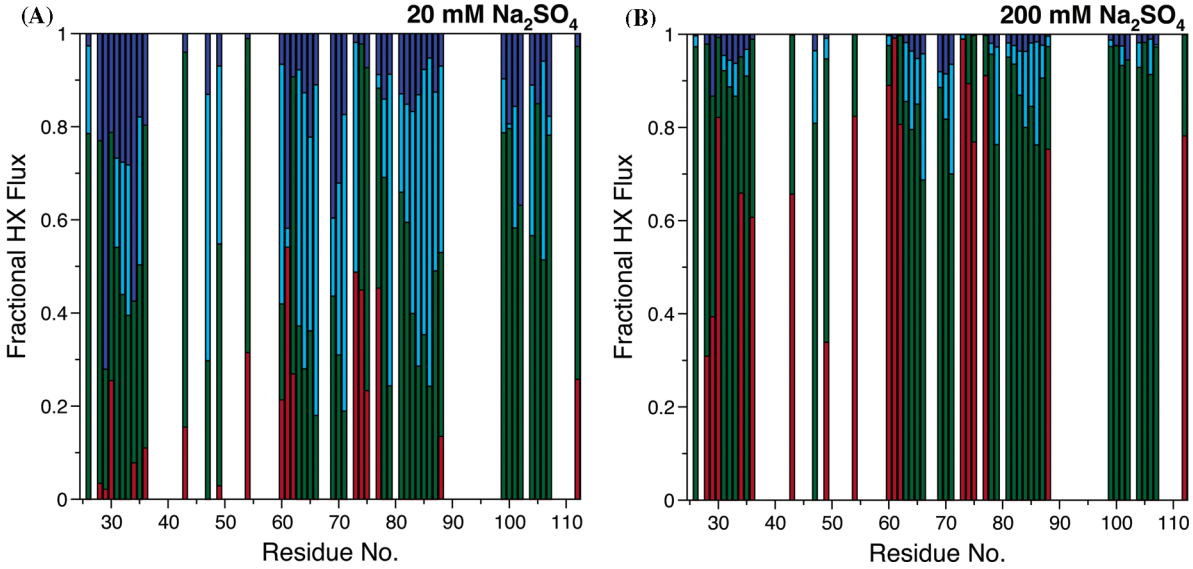

Figure 4. Fractional amide HX flux plots for P protein refolded in 20 mM Na_2SO_4 (A) and 200 mM Na_2SO_4 (B). The four colors correspond to the four specific HX pathways highlighted in Scheme 2. Dark blue bars represent HX through the global unfolding pathway D; light blue bars represent exchange through the local unfolding reaction from the unliganded N state. Green and red bars reflect global and/or local opening reactions from the singly liganded state, NL, and the doubly liganded state, NL_2, respectively. The fractional HX flux through NL_2, NL, N, and D were calculated using eqs 9 through 12.

measuredin the presence and the absence of ligand under native conditions. It is assumed that amides at, or near, the protein interaction surface would experience a reduction in the apparent HX rate upon binding the ligand. Ligand binding could result in the formation of new hydrogen bonds between the protein and the ligand or simply bury the amide groups from solvent.[41,43,44] However, reduced HX rates generally occur at sites proximate to *and* distant from known interaction surfaces.[38−45,47] Accordingly, the reduction in k_{obs} for these distant sites has been interpreted as evidence for ligand-induced conformational changes and/or the presence of intramolecular crosstalk patterns within the protein. However, an alternative interpretation exists to explain a reduction in k_{obs} upon ligand binding. Specifically, ligand alters the population of the states that give rise to exchange, whether or not these states include bound ligands. If HX occurs primarily through the free state, the addition of ligand decreases the HX rate because the concentration of the free species is reduced. Thus, there may be no correlation between the protein interaction regions or ligand-induced conformational changes and k_{obs}.[8,9] We find this alternative interpretation to most accurately describe the observed HX patterns for most observable residues of P protein.

In P protein, the conclusion that HX patterns do not reveal protein−sulfate interfaces is consistent with several observations. First, sulfate is a small ligand occupying a solvent accessible surface area of ∼100 Å^2,[48] which is insignificant compared to the ∼6800 Å^2 of solvent accessible surface area in folded P protein. Second, sulfate binds to the side-chain functionalities at the protein surface, while protected amides are solvent inaccessible. Third, there is not a significant increase in the overall population of the doubly liganded (or bound) state, NL_2, in the current experiments. The fraction of NL_2 rises from 99.95% to 99.995% over the range from 20 mM to 200 mM Na_2SO_4. (Note that these estimates were calculated assuming four species, NL_2, NL, N, and D, are present under the experimental conditions.) Fourth, the slow-exchanging amides do not map to the region of the known sulfate-binding site. The protected amides principally map to sites on the central β-sheet and α-helices 2 and 3. These regions constitute the "back" face of P protein; the secondary structural elements that stabilize the protein core are located on this face.[16] In contrast, the sulfate binding regions are located on the opposite face of the central β-sheet and on the sheet's edge.[16] Fifth, no significant changes are observed in the HSQC NMR spectrum at the different sulfate concentrations (data not shown). The implicit assumption is that an induced conformational change would alter the chemical shift environment of specific amides in a concerted, ligand-dependent manner. Thus, sulfate-dependence of k_{obs} cannot be interpreted by the traditional explanations.

HX experiments are very sensitive to poorly populated states.[5,6,20] In the current studies, the poorly populated states include the singly liganded ensemble (NL), the free folded ensemble (N), and the free denatured ensemble (D). Increasing sulfate concentration from 20 mM to 200 mM decreases the population of NL by a factor of 10 and the populations of N and D by a factor of 100. If the primary pathway of HX is through any of these states, then k_{obs} is expected to decrease. This expectation is met by many residues in P protein whose HX is principally through N and NL in 20 mM sulfate and through NL in 200 mM sulfate. Thus, the reduction in k_{obs} upon further ligand binding does not reflect any structural changes within the protein−ligand complex per se but rather the effect of ligand on the most exchange-competent populations. This phenomenon was observed by Chakshusmathi et al. who attributed the large difference in HX rate between RNase A and RNase S to the presence of small populations of the

(43) Williams, D. C., Jr.; Benjamin, D. C.; Poljak, R. J.; Rule, G. S. *J. Mol. Biol.* **1996**, *257* (4), 866−76.
(44) Williams, D. C., Jr.; Rule, G. S.; Poljak, R. J.; Benjamin, D. C. *J. Mol. Biol.* **1997**, *270* (5), 751−62.
(45) Wang, C.; Pawley, N. H.; Nicholson, L. K. *J. Mol. Biol.* **2001**, *313* (4), 873−87.
(46) Massiah, M. A.; Saraswat, V.; Azurmendi, H. F.; Mildvan, A. S. *Biochemistry* **2003**, *42* (34), 10140−54.
(47) Emerson, S. D.; Palermo, R.; Liu, C. M.; Tilley, J. W.; Chen, L.; Danho, W.; Madison, V. S.; Greeley, D. N.; Ju, G.; Fry, D. C. *Protein Sci.* **2003**, *12* (4), 811−22.
(48) Marcus, Y. *Biophys. Chem.* **1994**, *51* (2−3), 111−127.

dissociated fragments that compose RNase S, S peptide, and S protein.[8] This conclusion is in stark contrast to an earlier interpretation that the internal dynamics of the two ribonucleases are dramatically different despite their structural and enzymatic similarity.[49] Wildes and Marqusee find the ligand dependence of HX to be predominantly dependent upon the concentration of free protein even under conditions that favor the bound c-Src SH3 domain−peptide complex.[9] Furthermore, the sites that do exchange through the bound state do not correlate with regions that undergo other known ligand-induced changes for this complex.[45,50] Therefore, the ligand-dependence of k_{obs} may *not* reflect direct or indirect structural changes due to the protein−ligand interaction. Rather, this experiment may reflect the fact that ligands stabilize proteins and thereby perturb exchange pathways. Nevertheless, under appropriate conditions HX can be successfully used to identify ligand binding sites or ligand-induced conformational change (see below).

Ligation-State HX Is a Powerful Tool To Probe the Structural and Energetic Properties of Poorly Populated States within the Native Ensemble. P protein is categorized as an intrinsically unstructured protein because (1) it lacks the spectral characteristics of folded proteins when purified to homogeneity and (2) it lacks an unfolding transition at elevated temperatures.[13] However, P protein refolds to the known compact mixed α/β conformation[16−18] upon the addition of small anionic ligands such as sulfate. Moreover, only two states, D and NL_2, are predominantly populated at any sulfate concentration, thus coupled folding and binding is a two-state transition.[13] Nevertheless, the populations of other states such as NL, N, and perhaps even DL and DL_2 are not zero. Previously, we probed the structural and thermodynamic properties of N through the addition of trimethylamine *N*-oxide, TMAO.[13,19] However, this technique required the use of molar amounts of osmolyte, which has significant experimental limitations such as protein aggregation, solvent viscosity, and pH effects. Here, we studied the ligand dependence of HX to dissect the structural and energetic characteristics of the poorly populated intermediates. The principal advantage of this technique is the ability to extract residue specific information on the mechanism of the HX reaction. Moreover, this technique detects the regions of high stability within the poorly populated ensembles under native conditions.

Three primary HX pathways exist for a given amide in sulfate-folded P protein (Scheme 2). These pathways correspond to opening reactions from NL_2, NL, and N. Formally, these opening reactions can proceed either through various local or subglobal opening reactions at a particular amide or, alternatively, through global unfolding to DL_2, DL, or D, respectively. Using Scheme 2, a simple model can be derived to describe the ligand dependence of k_{obs}, or protection factors (eq 8). A plot of the HX data in a double reciprocal plot, PF^{-1} versus $K_d/[L]$, permits the facile determination of the opening equilibrium constants from the various bound and free states: K_{op}^{2L}, K_{op}^{L}, and K_{op}. Remarkably, ligation-state HX can extract information on equilibrium constants whose free energies differ by ~7.5 kcal/mol. This range corresponds to favorable opening reactions from the free state N (average $\Delta G_{op} \sim -2.7$ kcal/mol) to unfavorable opening reactions from the doubly liganded state NL_2 (average $\Delta G_{op} \sim +4.7$ kcal/mol).

Another unique aspect of this experiment is the ability to extract information about the fractional HX flux through the various pathways. The HX pathway with the lowest free energy should dominate the fractional flux of exchange. Using our model, we find the equilibrium constant for opening from the unbound states, K_{op}, to be several orders of magnitude greater than that for the bound states, K_{op}^{L} and K_{op}^{2L} (Table 1). Interestingly, ΔG_{op} from D and N are negative. Thus, it may seem that HX should occur through these favorable opening pathways. However, when the presence of ligand strongly favors the bound states, a significant portion of HX occurs through these more populated states; this is particularly true for P protein in 200 mM Na_2SO_4 (see Figure 4B). Consequently, many amide hydrogens are apparently able to access the high-energy fluctuations that lead to exchange from NL or NL_2. At ligand concentrations closer to the K_d than studied here (but still well above saturation), the predominant exchange mechanism is through the free states because the population of these states is high enough to compete with the much better protected liganded states. The addition of ligand provides a way to specifically sample high-energy, local unfolding reactions that are not significant at low ligand concentration. This ability of ligation-state HX experiments to uncover "masked" high-energy local unfolding reactions has been previously noted.[9]

Residue-specific information on the conformational properties of high-energy intermediate ensembles is another important feature of ligation-state exchange. The structural properties of the N state of P protein are inaccessible by standard spectroscopic techniques because the equilibrium population of N is at most 5×10^{-6} under conditions that favor the folded protein. Furthermore, D is typically the highest energy state that is sampled under standard native-state HX experiments.[34,51] However, using ligation-state HX exchange of some residues in P protein can be assigned to local fluctuations in the N state (light blue bars, Figure 4A). Furthermore, there are portions of P protein that are protected in N, leading to exchange via global unfolding. Thus, regions of global vs local protection within the N ensemble can be identified. Figure 5 highlights the residues that preferentially (i.e., ≥50%) exchange through the global unfolding pathway, D, in the free state. Interestingly, several of the amides map to residues whose side chains are involved in a hydrophobic cluster between the tight turn linking β-strands 1 and 2 (N28−F31) and several residues within α-helix 3 (K100, S102, L106, and R108) (Figure 5). Note there is no simple relationship between the residues that are partially protected in the N ensemble and the observed exchange rates. Thus, the highlighted regions do not correspond to the "slow-exchanging core"[33] of P protein. Kinetic protein folding experiments are necessary to determine whether the cluster of preferentially protected amides in N corresponds to an early folding intermediate, as has been seen for other proteins.[52−55] Indeed, the mechanism of P protein folding has yet to be determined. However, it would be intriguing if the folding

(49) Dong, A.; Hyslop, R. M.; Pringle, D. L. *Arch Biochem. Biophys.* **1996**, *333* (1), 275−81.
(50) Cordier, F.; Wang, C.; Grzesiek, S.; Nicholson, L. K. *J. Mol. Biol.* **2000**, *304* (4), 497−505.
(51) Chamberlain, A. K.; Handel, T. M.; Marqusee, S. *Nat. Struct. Biol.* **1996**, *3* (9), 782−7.
(52) Raschke, T. M.; Marqusee, S. *Nat. Struct. Biol.* **1997**, *4* (4), 298−304.
(53) Krishna, M. M.; Lin, Y.; Mayne, L.; Englander, S. W. *J. Mol. Biol.* **2003**, *334* (3), 501−13.
(54) Lu, J.; Dahlquist, F. W. *Biochemistry* **1992**, *31* (20), 4749−56.
(55) Jennings, P. A.; Wright, P. E. *Science* **1993**, *262* (5135), 892−6.

Figure 5. Residues protected in the high energy unliganded N ensemble mapped onto the P protein crystal structure[16] (Protein Data Bank code 1A6F). Highlighted in orange are the amino acids that preferentially exchange (≥50%) through the global unfolding pathway (through D) from the free state, N. Several residues protected in N localize to the tight turn between β-strands 1 and 2 and α-helix 3. The side chains for N28, Q30, F31, S102, and L106 are shown. Note that the population of N ranges from 5×10^{-6} to 5×10^{-8} as sulfate increases from 20 mM to 200 mM Na_2SO_4.

nucleus uncovered by ϕ-analysis[56] has any correlation to these protected sites in N.

Ligation-state HX permits the characterization of the regions that are protected within poorly populated high-energy intermediates. This method can potentially serve as a probe of allosteric systems in which high-energy states correspond to active or inactive conformations.[2,3] Additionally, ligation-state HX provides unique experimental information that can be used to compare with theoretical models that predict the existence of poorly populated conformational ensembles.

Simple Test To Determine whether Ligand-Based Changes in HX Kinetics Can Be Used To Map a Protein−Ligand Interface or Induced Conformational Change. NMR or mass spectrometry-based HX has been used in the past to identify regions of interaction in protein−ligand interactions.[37−47,57−61] The ligation-state HX results presented here and elsewhere[8,9] raise the question of whether exchange from states other than the bound complex might have contributed to the observed HX patterns in the previous studies. The analysis used here suggests two experimental tests that could be used to validate HX as a strategy for mapping protein−ligand interfaces in the future. First, for HX to be useful as an interface-mapping method, exchange must occur through local opening reactions in both the bound and free states. This can be verified by performing a native-state HX experiment, which compares exchange rates in low concentrations (~1 M) of urea with those in the absence of urea. If nonlocal conformational changes such as global or subglobal unfolding are coupled to the opening reaction, then the rates will not be the same in the presence and absence of urea. The second condition that must be satisfied is that exchange in the ligand-bound protein occurs through the bound state and not the free state. This can be verified by measuring HX at two ligand concentrations, both saturating. Ideally the two ligand concentrations would differ by a factor of at least 10. As can be seen from eq 8, only the fully liganded state affects the observed exchange rate in a ligand-independent way. Thus, if the HX rates observed in an interface mapping experiment are constant in the presence and absence of urea and at two different ligand concentrations, then the exchange mechanism is dominated by local exchange from the bound complex and it may be reasonable to assume that differences between free and bound HX rates reflect changes in solvent accessibility in the protein−ligand interface or regions of ligand-induced conformational change.[57]

We have shown that ligation-state hydrogen exchange can be used to measure the flux of hydrogen exchange through four different pathways in the P protein−sulfate complex. On this basis, we propose that ligation-state hydrogen exchange is a powerful method to study the thermodynamic coupling of conformational equilibria to ligand binding in other allosteric systems.

Acknowledgment. The authors were financially supported by NIH Grants GM45322 (T.G.O.) and GM08487 (C.H.H.). The authors thank Dr. Shallee T. Page for critically reading the manuscript and various members of the Oas laboratory for insightful discussions and advice.

Supporting Information Available: Table S1 lists the ^{15}N and ^{1}H chemical shift assignments of *B. subtilis* ribonuclease P protein refolded in 20 mM Na_2SO_4. Table S2 lists the best-fit HX rates (k_{obs}) for the 47 well-resolved slow-exchanging resonances at the four ligand concentrations. Figure S1 displays the fractional amide HX flux plots for P protein at the four ligand concentrations used in this study. Complete ref 15 is given. This material is available free of charge via the Internet at http://pubs.acs.org.

JA057279+

(56) Fersht, A. R. *Structure and Mechanism In Protein Structure: a guide to enzyme catalysis and protein folding*, 2nd ed.; W. H. Freeman and Company: New York, 1999; p 631.
(57) Mandell, J. G.; Falick, A. M.; Komives, E. A. *Proc. Natl. Acad. Sci. U.S.A.* **1998**, *95* (25), 14705−10.
(58) Engen, J. R.; Gmeiner, W. H.; Smithgall, T. E.; Smith, D. L. *Biochemistry* **1999**, *38* (28), 8926−35.
(59) Andersen, M. D.; Shaffer, J.; Jennings, P. A.; Adams, J. A. *J. Biol. Chem.* **2001**, *276* (17), 14204−11.
(60) Hamuro, Y.; Wong, L.; Shaffer, J.; Kim, J. S.; Stranz, D. D.; Jennings, P. A.; Woods, V. L., Jr.; Adams, J. A. *J. Mol. Biol.* **2002**, *323* (5), 871−81.
(61) Hoofnagle, A. N.; Resing, K. A.; Ahn, N. G. *Annu. Rev. Biophys. Biomol. Struct.* **2003**, *32*, 1−25.